Experimental Methods for Mobility and Surface Operations of Microgravity Robots

Benjamin Hockman[1], Robert G. Reid[2], Issa A. D. Nesnas[2], and Marco Pavone[1]

[1] Dept. of Aeronautics and Astronautics, Stanford University, Stanford, CA. 94305
{bhockman, pavone}@stanford.edu
[2] Jet Propulsion Laboratory, California Institute of Technology, Pasadena, CA. 91109
{rgreid, nesnas}@jpl.nasa.gov

Abstract We propose an experimental method for studying mobility and surface operations of microgravity robots on zero-gravity parabolic flights—a test bed traditionally used for experiments requiring strictly *zero* gravity. By strategically exploiting turbulence-induced "gravity fluctuations," our technique enables a new experimental approach for testing surface interactions of robotic systems in micro- to milli-gravity environments. This strategy is used to evaluate the performance of internally-actuated hopping rovers designed for controlled surface mobility on small Solar System bodies. In experiments, these rovers demonstrated a range of maneuvers on various surfaces, including both rigid and granular. Results are compared with analytical predictions and numerical simulations, yielding new insights into the dynamics and control of hopping rovers.

1 Introduction

Small Solar System bodies, such as comets, asteroids, and irregular moons, have become high-priority targets for planetary exploration [1,2]. Remote observations have suggested that many small bodies are topographically diverse both in composition and structure, requiring targeted measurements at multiple locations to characterize [2]. Accordingly, *controlled* surface mobility on small bodies was recently identified by the National Research Council as a high priority for NASA's technology development [3].

Controlled mobility in microgravity is challenging due to the almost complete lack of traction. Traditional wheeled vehicles, which rely on their weight to grip the surface, are restricted to extremely low speeds in microgravity and are highly susceptible to losing surface contact and flipping over when traversing uneven terrain. Several mobility techniques have been proposed for maneuvering in the microgravity environments found at the surface of small bodies. Specifically, *hopping* has been recognized by agencies such as NASA [4,5], ESA [6], RKA [7], and JAXA [8], as having many advantages over techniques such as wheeled and legged systems. In fact, two hoppers are currently en route to Asteroid 162173 Ryugu aboard JAXA's Hayabusa 2 spacecraft: a MASCOT lander developed by DLR [6] and three MINERVA landers [8], which are both equipped with momentum devices that allow them to hop, albeit with minimal control.

1.1 Hedgehog Hopping Rover

This paper considers, as a case study, a hopping rover developed by the authors called "Hedgehog," which utilizes internal actuation (via three mutually-orthogonal flywheels) to generate *controlled* directional hops in microgravity (see Fig. 1, left). Specifically, by applying an *internal* torque on the flywheels via motors and mechanical brakes, the chassis rotates and induces *external* reaction forces on the surface, producing ballistic hops (see Fig. 1, right). This mobility technique, as investigated in [9,10,11], offers a simple, yet uniquely capable, architecture for targeted mobility on small bodies (see overview video at: `http://youtu.be/bDmoqjNQAu8`). Specifically, [11] derives flywheel control laws for a variety of "motion primitives" (e.g., hopping, tumbling, and twisting) that have demonstrated a previously unobtained level of precision in simulations and ground-based experiments.
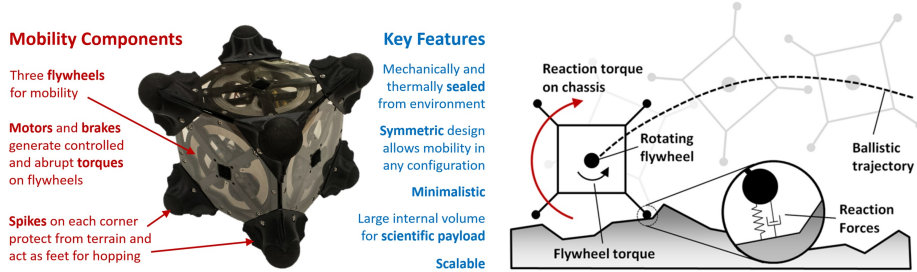

Figure 1. Left: Hopping rover prototype shown without avionics, covers, or solar panels. The cubic chassis encloses three orthogonal flywheels and is surrounded by eight compliant spikes on its corners. **Right:** By accelerating internal flywheels, surface reaction forces cause the rover to tumble or hop.

1.2 Experiments in Microgravity

One of the most challenging tasks when developing robotic systems for microgravity is *testing in relevant environments*. Here, and throughout this paper, "microgravity" refers to the small, but importantly, *non-zero* gravity (roughly 10^{-5} to 10^{-2} g's) exerted by a small body. At these scales, surface reaction forces are small and motion is slow, so it is not practical or comparable to test microgravity systems in $1\,\mathrm{g}$ environments (as can be done, for example, with Martian rovers). This is an issue for mobility systems as well as other surface operations such as excavation or anchoring devices. Instead, there have been various methods proposed for *emulating* reduced gravity on Earth, which can be roughly divided into two classes: (1) free-fall test beds, such as drop towers and parabolic flights, and (2) gravity-offloading test beds that aim to "counteract" the force of gravity.

Various gravity-offloading approaches have been demonstrated, including buoyancy tanks, air-bearing tables [9], passive counterweight mechanisms [9,10], and actively controlled tracking systems [11,12,13,14]. Gravity-offloading test beds generally allow for longer duration and less expensive tests than free fall chambers, but they typically introduce undesirable exogenous dynamics and/or restrict the system's range of motion. For the Hedgehog rover presented in Sect. 1.1, Hockman et al. developed a first-of-a-kind test bed at Stanford University, uniquely capable of tracking the Hedgehog's motion in 6 degrees of freedom (DoF) under dynamic force inputs [11]. It consists of an actively-controlled overhead 3-axis

gantry crane that tracks the translational motion of the Hedgehog at an effective 0.0005 - 0.005 g's, and a passive gimbal that allows the Hedgehog to freely rotate about all three axes (see Fig. 2). While this test bed has demonstrated effective tracking performance for some types of maneuvers such as small hops and tumbles, it has three inherent limitations: (1) it cannot track fast maneuvers such as more aggressive hops, (2) the added mass and inertia of the gimbal prevent accurate tracking of rotations about non-symmetric axes, and (3) it cannot offload the surface regolith's mass, which, especially for loose granular materials, can behave quite differently in microgravity.
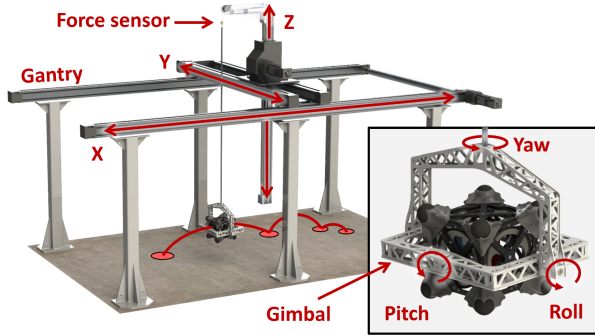
Figure 2. The Stanford 6 DoF microgravity test. The powered gantry tracks the translational motion of the Hedgehog, while allowing for free fall at sub-milli-g levels. The gimbal frame allows the Hedgehog to rotate in all three axes.

Statement of Contributions: The contributions of this paper are twofold: first, we propose a novel experimental method that utilizes zero-g parabolic flights—a test bed traditionally used for experiments requiring strictly *zero* gravity—for testing microgravity surface operations (Sect. 2). Our approach exploits the "gravity fluctuations" induced by turbulence on the aircraft to trigger experiments during windows of acceptable conditions. The proposed technique avoids many of the limitations observed in gravity-offloading test beds, and thus offers a complementary approach to testing robotic systems, such as Hedgehog, that are designed for microgravity environments. Second, we use this experimental procedure to evaluate the controllability of two Hedgehog prototypes performing various maneuvers on several rigid and granular surfaces. The results largely agree with predictions based on analytical and numerical models (Sect. 3). To the best of the authors' knowledge, these experiments constitute some of the first demonstrations of *controlled* hopping on a zero gravity aircraft.

2   Parabolic Flight Experiments

Parabolic flights offer a unique environment to conduct experiments in effectively reduced gravity, but they pose significant challenges for systems that require smooth and stable accelerations. During each parabola, disturbances caused by turbulence and control errors induce "gravity fluctuations" on the order of ± 0.03 g's. Figure 3 shows a representative example of time-series acceleration data collected on NASA's C9 aircraft. Brief periods of negative g's are particularly problematic for unrestrained robots that need to remain in contact with a surface (such as our Hedgehog), since they will inadvertently float away.

One solution is to "positively bias" the effective gravity such that it never goes negative. Typically, this can only be afforded for a small fraction of parabolas since multiple experimental payloads are flown on each flight, and most

require net-zero gravity. During zero-g parabolas, however, gravity fluctuations often produce brief periods with slightly positive gravity conditions that can be utilized for microgravity experiments. With this in mind, we propose an experimental method that systematically exploits these fluctuations to enable surface-interaction experiments with microgravity robotic systems.
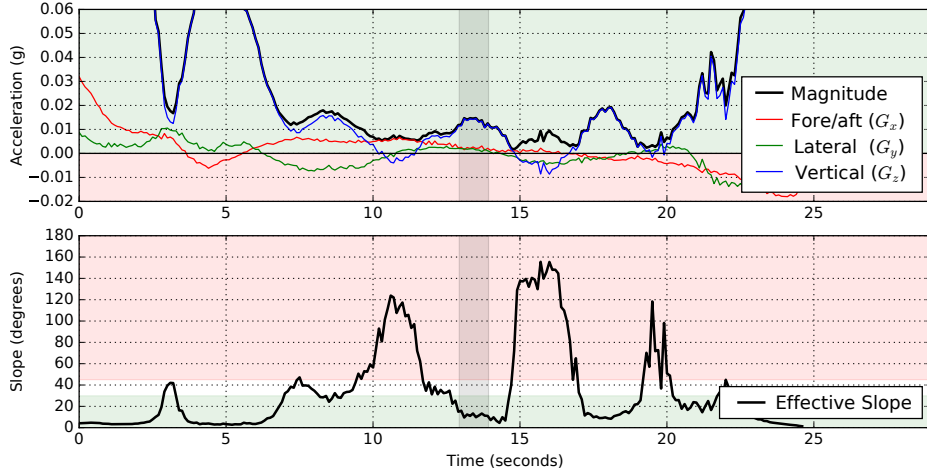
Figure 3. Example time-series acceleration data from C9 reduced gravity aircraft during a parabola. **Top:** Accelerations of the aircraft in the aircraft reference frame. **Bottom:** Effective slope of the experimental payload; $0°$ is horizontal, while $90°$ is sideways.

Our experimental setup is as follows (see Fig. 4): the Hedgehog prototype sits on the test surface and is restrained by a retractable arm that applies a gentle downwards force. An accelerometer, rigidly mounted to the floor of the aircraft, measures the transient accelerations and is used to automatically retract the arm and initiate each experiment when the resulting gravity conditions are deemed acceptable. An array of small cameras fixed inside the payload container track the Hedgehog's motion (position and attitude) with millimeter precision and high frame rates (240 Hz) via body-mounted fiducial markers. Some cameras were also focused on the surface to observe contact interactions.
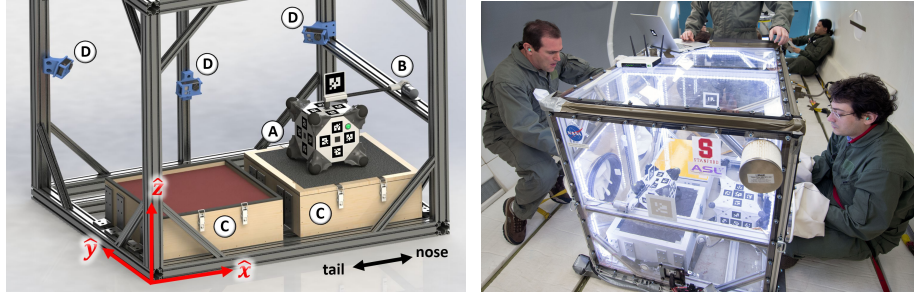
**Figure 4.** Experimental setup. **Left:** The Hedgehog (A) is held in place on the test surface (C) by an actuated arm (B). An array of five cameras (D) capture its motion as it hops within the container. **Right:** Photo of our experiments on NASA's C9 aircraft.

"Acceptable" gravity conditions for triggering an experiment should be tailored for the particular system being tested. Since Hedgehog actuates while in contact

with the surface, for example, we defined the triggering condition as the first point at which (1) the total acceleration magnitude is less than 0.02 g's (with a low-pass filter) *and* (2) the effective slope is less than 30° relative to the surface normal (to avoid sliding or tipping before actuation). The shaded region in Fig. 3 shows the time at which an experiment was triggered for that particular parabola. Historical acceleration data for the particular aircraft should be analyzed to validate the desired triggering condition and to predict the percentage of parabolas that would allow successful triggering. Thus, for experiments with flexible gravity requirements, there is an inherent trade between the acceptable parabola quality and probability of a trigger occurring.

To emulate a range of surface properties that rovers may encounter on small bodies, the experimental payload container in Fig. 4 was fitted with two boxes (labeled "C") that provided a total of four different test surfaces: a low-friction *Kapton tape* covering the (rigid) lid of one box, a high-friction *grip tape* on the other lid, a cohesive *comet regolith simulant* [15], and a low-cohesion *garnet sand* (see Fig. 5). The two rigid surfaces, "A" and "B," aim to mimic rocky or icy surfaces with varying degrees of "traction." The simulant "C," is a crushable material consisting of an aerated cement that mimics cohesive (yet friable) regolith. Its cohesive properties allowed it to be exposed during negative g's, unlike the garnet sand, "D."
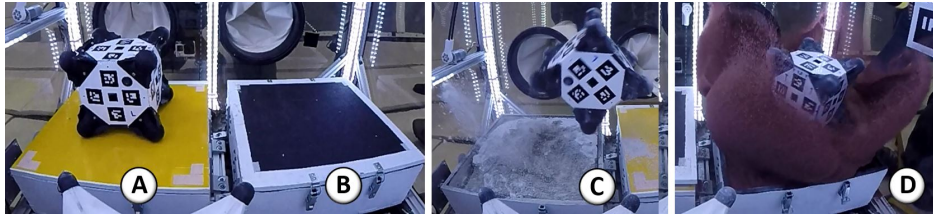
Figure 5. Test surfaces: (A) low-friction and (B) high-friction rigid surfaces, (C) crushable comet regolith simulant, and (D) granular, low-cohesion garnet sand.

3   Mobility Experiments

The experimental techniques discussed in Sect. 2 were used to evaluate the controllability of two Hedgehog prototypes performing maneuvers on various surfaces. Over the course of four flights, 74 of 190 parabolas resulted in successfully triggered mobility experiments. Of those, 64 were performed on three different surfaces in zero-g parabolas (0 ± 0.02 g), while 10 were performed on the garnet sand in positively-biased parabolas (0.03 ± 0.02 g). The remaining parabolas experienced unfavorable gravity conditions or technical difficulties (timing error of the arm release and hop trigger, operator error, software bugs, and wireless interference from aircraft communication). Most parabolas were utilized for hopping experiments, but a few were also used to test more precise maneuvers such as tumbling and twisting. A video compilation of several maneuvers can be found at http://web.stanford.edu/~pavone/iser16.

3.1   Predictive Modeling and Analysis

Several numerical and analytical models have been designed to study the dynamics of this mobility platform and to derive control laws for executing deliberate

maneuvers (see [11] for details). By simplifying the rover's geometry, and assuming instantaneous momentum transfer with no slipping during contact, the two models in Fig. 6 A and B allow control laws to be derived *analytically* from rigid body dynamics and angular momentum arguments. These control laws depend on the rover's geometric and inertial properties, as well as its resting pose on the surface. For hopping with high-torque brakes, these control laws map a desired takeoff velocity vector to the prerequisite angular speeds of the flywheels.
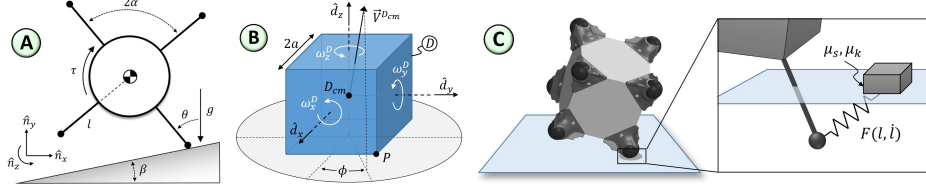
Figure 6. Dynamic Models. **A:** 2D model used to derive control laws for *single-axis* hops [11]. **B:** Hedgehog is modeled as a cube pivoting on one of its corners, which is used to derive control laws for *directional* hops [11]. **C:** A numerical contact model assumes Coulomb friction and arbitrary penetrating force function.

To study more realistic dynamics, a penetrating contact model was designed to allow slip and surface deformation that is numerically integrated to solve for the Hedgehog's trajectory (see Fig. 6C). By varying the friction coefficients (μ_s, μ_k) and the penetration force function (F) this "elastic sliding block" model can approximate a wide variety of surface properties. For most rigid (or near-rigid) surfaces, a damped elastic model works well (i.e. $F = kl + b\dot{l}$), but more complex nonlinear models can also be devised to capture surface deformation effects. While a numerical approach does not yield analytical control insights, it is useful for understanding motion on irregular surfaces and the response in subsequent surface collisions. These models can now serve as a basis for comparison with data collected on microgravity experiments.

3.2   Hopping Experiments

Since the dynamics of a hopping rover in ballistic flight are deterministic (for an airless body with known spin and gravity model), we can characterize the resulting trajectory with three parameters describing its initial launch velocity vector: speed (v_h), elevation angle (θ_h), and azimuth angle (ϕ_h). These parameters are extracted from the visual tracking data by fitting a parabola to the time-series position measurements of the Hedgehog's mass center for the first 20 cm of its trajectory after takeoff. The observed hop vectors can then be compared with predictions obtained by inputting the observed flywheel speeds into our models.

The results in Fig. 7 show predicted values on the horizontal axis and measured trajectory data on the vertical axis. Each data point represents a trajectory resulting from a particular set of flywheel speeds. The analytical model used for comparison in the left plots is shown in Fig. 6B, and the numerical model for the right plots, in Fig. 6C. Overall, there was strong agreement between the experimental and model-generated data with mean absolute errors of about 10% for speed, and 5° for elevation and azimuth angles. It is important to note that Hedgehog experienced slight drift before actuation on many of these maneuvers, such that its initial state was not exactly grounded and stationary, as assumed
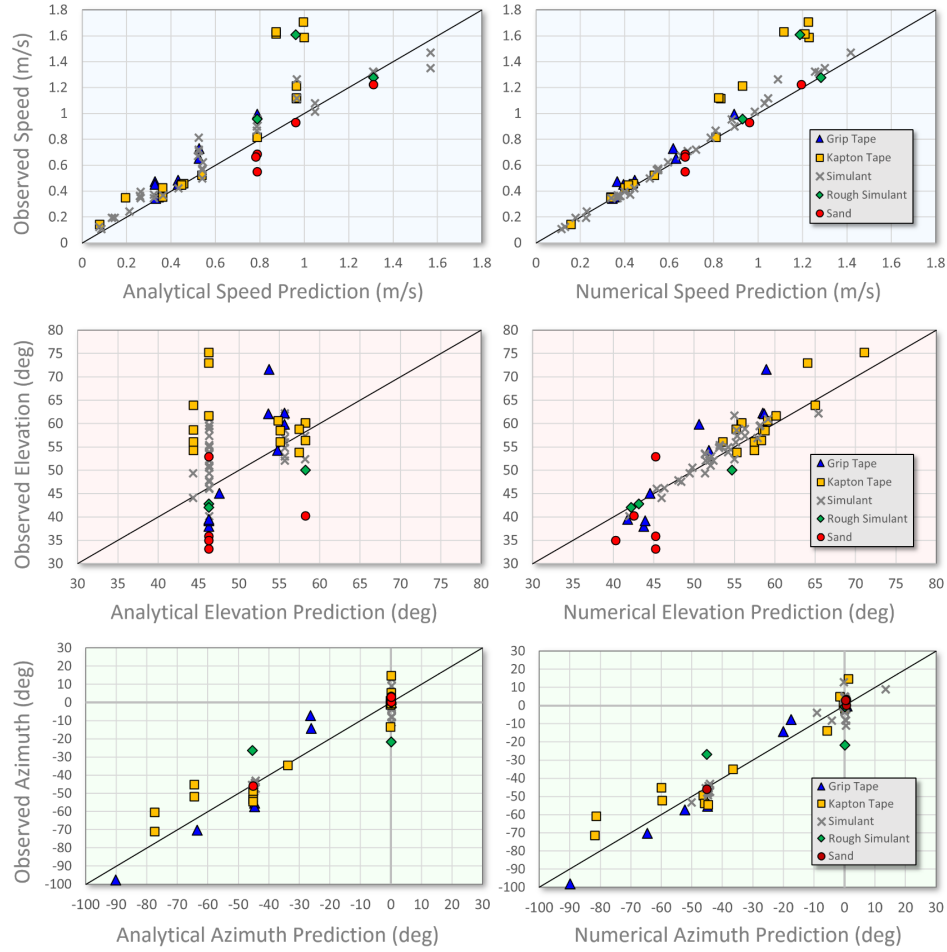
Mean Absolute Errors (MAE)

	#	Speed		Elevation		Azimuth	
		Analytical	Numerical	Analytical	Numerical	Analytical	Numerical
Grip Tape ▲	9	17.7 %	9.6 %	6.2°	4.8°	7.8°	5.0°
Kapton Tape ■	15	24.3 %	16.5 %	9.8°	2.3°	7.2°	6.6°
Simulant ✕	33	16.7 %	5.1 %	5.1°	1.5°	3.7°	3.3°
Rough Simulant ◆	3	22.2 %	11.2 %	4.6°	1.6°	13.2°	12.2°
Sand ●	5	17.1 %	5.7 %	9.7°	6.9°	1.9°	1.8°
Total	**65**	**18.4 %**	**7.8 %**	**6.6°**	**2.4°**	**5.3°**	**4.7°**

Figure 7. Experimental trajectory data (speed, elevation, and azimuth) for 65 hopping maneuvers on 5 surfaces (see Fig. 5) compared with predictions based on an analytical model (left plots) and a numerical model (right plots). "Rough simulant" corresponds to a few experiments in which the comet regolith simulant was highly fractured and uneven. Predictions and observations that are in agreement lie along the black lines with slope 1. The table of mean absolute errors summarizes these results.

by the analytical model. Therefore, it is not surprising that the numerical model, *which is simulated from the actual measured initial states* and accounts for the varying surface properties, exhibits stronger agreement with the data than the less-informed analytical model.

Examining systematic bias in the data can help to identify unmodeled effects and make improvements. For example, the clustering of analytical elevation predictions at 45° reflects the no-slip and instantaneous momentum transfer assumptions for single-axis hops, which are not realizable for lower friction surfaces and brakes with limited torque. If, however, information about the surface friction is known *a priori*, the control law can be adjusted to reflect the higher expected elevation ($\theta_{\mathrm{h}} \approx \cot^{-1} \mu$). Also, contact interactions with loose granular regolith, which is essentially "fluidized" by microgravity, does not adhere well to either the pin-jointed spike contact assumption or the numerical contact model (such as overestimated hop elevation on sand in Fig. 7); it will be the subject of future work. Finally, it is suspected that the high-speed outliers can be attributed to a temporary hardware issue with one of the prototype's braking mechanisms.

3.3   Tumbling Experiments

Tumbling is simply a less energetic form of hopping, whereby the Hedgehog rotates about a pair of spikes without losing ground contact, nominally rotating 90° and translating one body length. For this single-flywheel maneuver, an upper and lower bound on the control input are derived in [11], which correspond to the speed at which the Hedgehog would rotate too fast and lose surface contact and the speed at which it would just barely tip over, respectively.

$$\omega_{\max} = \sqrt{\frac{g \cos \beta}{\eta^2 l \cos \alpha}}, \qquad \omega_{\min} = \sqrt{\frac{2m_{\mathrm{p}}gl(1 - \cos(\alpha + \beta))}{\eta I_{\mathrm{f}}}}. \tag{1}$$

These bounds are functions of the Hedgehog's inertial and geometric properties ($m_{\mathrm{p}}, I_{\mathrm{f}}, \eta, \alpha, l$), its initial pose ($\beta$), and gravity ($g$) (see [11] for details). However, due to the need to maintain continuous ground contact over a longer time period, tumbling maneuvers could not exploit brief gravity transients and were therefore restricted to positively-biased parabolas. Table 1 summarizes data for the two tumbles performed.

Trial	Surface	Inclination*	$\omega_{\min}$ (rpm)	$\omega_{\max}$ (rpm)	ω (rpm)	Success?
1	sand	$-10.7°$	1451	2937	1968	Yes
2	sand	$-22.7°$	255	837	274	Yes

Table 1. Data from two successful tumbling experiments on sand at about 0.035 g's. Note that the measured flywheel speed (ω) is indeed between the predicted minimum and maximum bounds (see Eq. 1). *Negative inclination indicates a "downhill" tumble.

While the data is sparse, a few insightful observations were made. For one, on loose granular media, the leading spikes tend to sink into the surface, which shifts the pivoting axis inward and effectively shortens the modeled spike length (l). Also, faster tumbles have a higher chance of producing undesirable rebounds upon impact. However, both of these incidental effects can be mitigated by operating in the lower speed range (e.g. 10% higher than $\omega_{\min}$).

4 Main Experimental Insights

Despite the negative gravity fluctuations, accelerometer data indicates that approximately 40% of parabolas in NASA's C-9 aircraft yield acceptable conditions for brief microgravity mobility experiments, proving that parabolic flights can be a viable test bed for microgravity robotic systems. Moreover, for other short-duration microgravity experiments that can be executed in quick succession, some parabolas may offer multiple opportunities to collect data. This was not possible with our Hedgehog prototypes, as they require time to accelerate the flywheels.

An intuitive way of understanding the hopping uncertainty is by considering the transfer of angular momentum from the flywheel to the Hedgehog, which is assumed to be conserved *about the pivoting spike(s)* in the control analysis. Indeed, among the hops that did not experience initial drift, the momentum saw a mean loss of only 7%. Importantly, however, this angular momentum can be decomposed into the sum of linear ($\boldsymbol{r} \times \boldsymbol{p}$) and rotational ($\boldsymbol{I} \cdot \boldsymbol{\omega}$) components, which can be thought of as the "speed" and "spin" of the Hedgehog. Since we are primarily concerned with the translational trajectory, it is important to understand what portion of the flywheel momentum is converted to linear motion of the mass center. In theory, for the pin-jointed contact model in Fig. 6A, linear and rotational momentum should be in fixed proportions, $ml^2 \propto I$, respectively, where m is the mass, l is the spike length, and I is the centroidal inertia. However, there are certain conditions for which these proportions can be *distorted*. Contact elasticity, for example, can induce a recoil effect as the spikes push against the surface, which reduces the forward spin and increases the speed of the hop. In extreme cases, this may even induce a counter-rotation, and thus, *much* faster hops. Although elasticity generally yields more efficient hops, it is also less predictable, suggesting that more damping/shock-absorbing spikes may be favorable.

Surface *slip*, on the other hand, has the opposite effect: on low-friction surfaces, the planted spikes tend to slip, or "sweep" under the hopper and incur faster spinning, yet slower hops (which also increases the hop elevation to $\theta_\mathrm{h} \approx \cot^{-1}\mu$). That said, a smooth Coulomb friction model is likely a gross oversimplification for the deformable and irregular surfaces likely to be found on small bodies. For example, the comet regolith simulant described in Sect. 2 is smooth to the touch but often crushed under the pressure of the spikes during a hop, creating a secure foothold that prevents slip. Thus, future work will consider alternative spike designs that include small features to penetrate and grip the surface.

In addition to hopping and tumbling, *twisting* maneuvers were also tested whereby the Hedgehog spins about its vertical axis. This can be leveraged in a controlled way to rotate by some small angle, as discussed in detail in [11]. This was only tested once on sand in 0.03 g's, which produced a small angular shift as expected. While not directly useful for controlled mobility, *aggressive* twisting maneuvers (e.g. twists that result in more than one full revolution) could be utilized to energetically escape when embedded in loose regolith. One such maneuver was executed while the Hedgehog was partially embedded in the garnet sand; it ejected all sand within its swept radius and the Hedgehog was launched vertically.

The various ways in which surface properties can affect mobility performance raises an interesting question for further research: the inverse problem—that is—given some known control input and corresponding force on the surface, how can information about physical properties of the surface be extracted from the

dynamic response. Even constraining bulk properties, such as regolith density, depth, and cohesion, would provide useful information for mission designers and planetary scientists alike.

In the broader context of motion planning and navigation on small bodies, the ultimate goal is to reach designated targets, and the controllability of hopping, demonstrated in this paper, is simply one factor that enables this. The dynamics of subsequent bouncing and the physical and topographical properties of the environment also play a critical role. Thus, it is perhaps more important to characterize the *uncertainty* of a hop than it is to further refine its accuracy with more complex control regimes. The experiments enabled by our method for strategic microgravity testing—and the improved models they inspire—offer unique insight towards achieving this goal.

References

1. "Decadal Survey Vision and Voyages for Planetary Science in the Decade 2013–2022," National Research Council, Tech. Rep., 2011.
2. J. C. Castillo Rogez, M. Pavone, I. A. D. Nesnas, and J. A. Hoffman, "Expected Science Return of Spatially-Extended In-situ Exploration at Small Solar System Bodies," in *IEEE Aerospace Conference*, Big Sky, MT, Mar. 2012, pp. 1–15.
3. "NASA Space Technology Roadmaps and Priorities: Restoring NASA's Technological Edge and Paving the Way for a New Era in Space," National Research Council, Tech. Rep., 2012.
4. R. Jones, "The MUSES–CN rover and asteroid exploration mission," in *22nd International Symposium on Space Technology and Science*, 2000, pp. 2403–2410.
5. P. Fiorini and J. Burdick, "The Development of Hopping Capabilities for Small Robots," *Autonomous Robots*, vol. 14, no. 2, pp. 239–254, 2003.
6. C. Dietze, S. Herrmann, F. Kuß, C. Lange, M. Scharringhausen, L. Witte, T. van Zoest, and H. Yano, "Landing and mobility concept for the small asteroid lander MASCOT on asteroid 1999 JU3," in *International Astronautical Congress*, 2010.
7. R. Z. Sagdeev and A. V. Zakharov, "Brief History of the Phobos Mission," *Nature*, vol. 341, no. 6243, pp. 581–585, Oct. 1989.
8. "JAXA Hayabusa mission," JAXA, Tech. Rep., 2011, available at http://hayabusa.jaxa.jp/e/index.html.
9. R. Allen, M. Pavone, C. McQuin, I. A. D. Nesnas, J. C. Castillo Rogez, T.-N. Nguyen, and J. A. Hoffman, "Internally-Actuated Rovers for All-Access Surface Mobility: Theory and Experimentation," in *Proc. IEEE Conf. on Robotics and Automation*, Karlsruhe, Germany, May 2013, pp. 5481–5488.
10. R. G. Reid, L. Roveda, I. A. D. Nesnas, and M. Pavone, "Contact Dynamics of Internally-Actuated Platforms for the Exploration of Small Solar System Bodies," in *i-SAIRAS*, Montréal, Canada, Jun. 2014, pp. 1–9.
11. B. Hockman, A. Frick, I. A. D. Nesnas, and M. Pavone, "Design, Control, and Experimentation of Internally-Actuated Rovers for the Exploration of Low-Gravity Planetary Bodies," in *Conf. on Field and Service Robotics*, Toronto, Canada, 2015.
12. M. Chacin and K. Yoshida, "A Microgravity Emulation Testbed for Asteroid Exploration Robots," in *Proc. i-SAIRAS*, 2008.
13. B. H. Wilcox, "ATHLETE: A limbed vehicle for solar system exploration," in *Aerospace Conference, 2012 IEEE*.   IEEE, 2012, pp. 1–9.
14. P. Valle, L. Dungan, T. Cunningham, A. Lieberman, and D. Poncia, "Active Response Gravity Offload System," 2011.
15. E. M. Carey, G. H. Peters, L. Chu, Y. M. Zhou, B. Cohen, L. Panossian, M. Choukroun, J. R. Green, P. Backes, S. Moreland, and L. R. Shiraishi, "Development and characteristics of mechanical porous ambient comet simulants as comet surface analogs," in *Lunar and Planetary Science Conference*, 2016.